



# University of HUDDERSFIELD

## University of Huddersfield Repository

Shih, Jou-Yi, Kostovasilis, Dimitrios, Bezin, Yann and Thompson, D.J.

Modelling options for ballast track dynamics

### Original Citation

Shih, Jou-Yi, Kostovasilis, Dimitrios, Bezin, Yann and Thompson, D.J. (2017) Modelling options for ballast track dynamics. In: 24th international congress on sound and vibration, 23-27th July 2017, London. (Unpublished)

This version is available at <http://eprints.hud.ac.uk/id/eprint/31976/>

The University Repository is a digital collection of the research output of the University, available on Open Access. Copyright and Moral Rights for the items on this site are retained by the individual author and/or other copyright owners. Users may access full items free of charge; copies of full text items generally can be reproduced, displayed or performed and given to third parties in any format or medium for personal research or study, educational or not-for-profit purposes without prior permission or charge, provided:

- The authors, title and full bibliographic details is credited in any copy;
- A hyperlink and/or URL is included for the original metadata page; and
- The content is not changed in any way.

For more information, including our policy and submission procedure, please contact the Repository Team at: [E.mailbox@hud.ac.uk](mailto:E.mailbox@hud.ac.uk).

<http://eprints.hud.ac.uk/>

# MODELLING OPTIONS FOR BALLAST TRACK DYNAMICS

Jou-Yi Shih, Dimitrios Kostovasilis, Yann Bezin

*Institute of Railway Research, University of Huddersfield, Huddersfield, UK*  
email: j.shih@hud.ac.uk

David J. Thompson

*Institute of Sound and Vibration Research, University of Southampton, Southampton, UK*

Accurate modelling of railway ballasted track dynamics is an important issue for a variety of applications such as the assessment of wheel/rail contact force and critical speed of the vehicle. Track design and assessment against safety and stability criteria can now rely on a number of advanced and validated dynamic models. However, there is a large range of different models that can be used to predict ballasted track dynamics. They vary from fast and simple rigid multi-body models as used in commercial Multibody System approach (MBS) vehicle dynamics calculations, to more complex and expensive three-dimensional (3D) Finite Element (FE) models. This paper investigates the influence of different modelling options up to 2000 Hz for characterising ballasted track dynamics with the aim of providing guidelines for simplifying the model and summarising the advantages and limitations of each option. Five different models, a two-degrees-of-freedom (2 dof) multi-body track model, 2D FE model, 3D FE models with/without consideration of sleeper flexibility, and a 3D FE track model with homogeneous ballast layer are used to represent the ballasted track as a two-layer support and compared against an analytical solution. Consideration is given to the flexibility of the sleepers, inclusion of ballast density and geometry, element discretization level and FE model length. Equivalent parameters to convert input data from one model to another are summarized.

Keywords: Ballast track, Finite element method, discrete sleeper, flexible sleeper, rigid multi-body track

---

## 1. Introduction

Numerical simulation of vehicle/track interaction dynamics has become an important tool for ensuring adequate vehicle performance in terms of vehicle stability, running safety, damage and irregular wear of the wheel and rail surface [1]. As a result, an accurate numerical tool plays an important role in assessing the design and performance of vehicles in order to improve the running stability and reduce the maintenance cost. Commercial MBS software has been commonly used for this assessment, and can include very complex vehicle models including friction elements, non-linear bushings, air-springs and so on. However, track model is usually assumed to be rigid or rigid multi-body that will lead to overestimates of the vehicle critical speed and underestimates of the dynamic contact forces [2,3]. Furthermore, consideration of a flexible track has a significant influence for the stress and frictional power density distributions occurring in the wheel/rail contact [3]. As a result, track dynamic behaviour plays an important role for the assessment of vehicle dynamics and contact mechanics. The aim of the present work is focus on the track modelling in order to have better understanding of track behaviour that can lead to better prediction of vehicle/track interaction dynamics.

Ballasted track is considered here, due to that fact that it is the most common commercial track form used all over the world. The ground beneath the ballast is assumed to be rigid in the present work. This leads to a good prediction of the dynamic behaviour of the track, except for cases where the ground stiffness is very low [4] provided that suitable properties are used for the ballast that

include the ground flexibility. The rail receptance calculated by frequency domain analysis from five different track models is analysed here in order to establish the most suitable model to be used, depending on the desired application. Even though similar studies can be found in literatures, procedure for converting a complex model to a simple model is still not clear. A guideline for relating the track parameters required for each model is provided and the benefits and limitations of each modelling option are discussed based on the frequency range of validity. FE and MBS models are used in the present work and validated against an analytical solution [5]. Even though an analytical solution is more efficient and does not have boundary and numerical issues, FE and MBS models are usually used for vehicle/track interaction modelling in order to account for nonlinear contact between wheel and rail. Investigation of the influence of different modelling options up to 2 kHz for characterising ballasted track dynamics is presented here. This limit is chosen in order to capture accurate dynamic behaviour for irregular running surfaces of the wheel and track components (0~1500 Hz [6]) and assessment of P1 (500~1000 Hz) and P2 (30~100 Hz) forces [7].

## 2. Numerical models

Five different models, including one multi-body track model and four FE models, are used to represent the ballasted track. This section gives a brief description of the various models used, as well as means of transforming the various track parameters to be used as an input for each model. The main track parameters used throughout this study are shown in Table 1. Here, the railpad damping represents a damping ratio of 0.1 for the second resonance frequency (~400 Hz). Similarly, the ballast damping represents a damping ratio of 0.5 for the first resonance frequency (~100 Hz).

Table 1: Two-layer track properties for discrete sleeper model [5]

Parameter	Value	Units
Rail mass per unit length, $\rho_r$	7850	kg/m <sup>3</sup>
Rail Young's modulus, $E$	$2.1 \times 10^{11}$	N/m <sup>2</sup>
Rail area, $A_r$	0.00763	m <sup>2</sup>
Rail second moment inertia, $I$	$3.055 \times 10^{-5}$	m <sup>4</sup>
Rail shear constant	0.4	
Railpad stiffness, $k_p$	$195 \times 10^6$	N/m
Railpad damping, $c_p$	$17.44 \times 10^3$	Ns/m
Total sleeper mass, $M_s$	325	kg
Sleeper spacing, $L_s$	0.65	m
Ballast stiffness per half sleeper, $k_b$	$65 \times 10^6$	N/m
Ballast damping per half sleeper, $c_b$	$114.5 \times 10^3$	Ns/m

The numerical models are compared with an analytical solution for the vibration of a discretely supported rail on a two-layer foundation obtained from [5].

### 2.1 Two-degree-of-freedom equivalent track model (Model 1)

A two-degree-of-freedom track model (Model 1) is shown in Fig. 1. The track is assumed to be symmetrical with respect to the longitudinal axis. Therefore, only half of the track is considered. This model only accounts for the mass of the rail and sleeper, and the stiffness of the railpads and ballast, with no consideration given for the bending properties of the rail, or the discrete nature of the supports. Such track models are widely used in MBS vehicle/track interaction software, known as ‘‘co-running’’ track models, as they are always following the wheel/rail contact position.

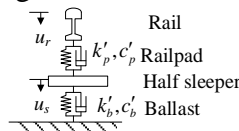


Figure 1: Two-degree-of-freedom equivalent track model (Model 1)

The model parameters are calibrated here in such a way as to match the low frequency response of the track, i.e. the static track stiffness, between the 2-dof model and the analytical solution. This is achieved by considering the effective length of the track that contributes to the response of the beam, given by the static track stiffness ( $K_{st}$ ) and the stiffness of an equivalent continuous support layer ( $k_s$ ) as follows [8]:

$$L_{eff} = K_{st} / k_s \tag{1}$$

where

$$k_s = \frac{k_p k_b}{L_s (k_p + k_b)}; K_{st} = 2\sqrt{2} (EI)^{1/4} k_s^{3/4} \tag{2}$$

Finally, the parameters for Model 1 can be obtained, here for the railpad stiffness for example, as:  $k'_p = k_p L_{eff} / L_s$ .

## 2.2 FE track models

### 2.2.1 Two-dimensional FE track model (Model 2)

Model 2 is a 2D FE track model, where half the track is considered with parameters listed in Table 1 (with half the sleeper mass), as shown in Fig. 2. The Timoshenko beam element (a 2-node beam element with consideration of shear flexibility) is used to represent the rail and the load is applied in the middle of the track model above a sleeper. For the sleeper, a point mass is used. Spring-dashpots are applied between the rail and the sleeper, and between the sleeper and the rigid foundation. The boundaries at either end of the rail are assumed to be free. As a result, an assessment of the boundary effect is required, which will be discussed in Section 3.1.3.

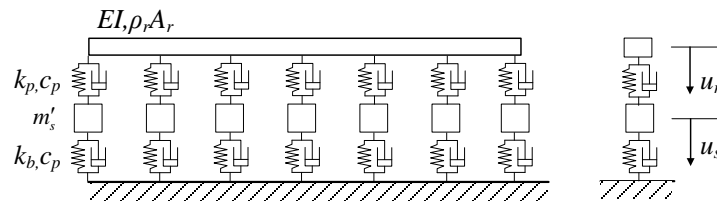


Figure 2: 2D FE ballasted track model (Model 2)

### 2.2.2 Three-dimensional FE track models (Models 3~5)

A full track model is considered for all 3D models except Model 5, which is simplified in order to save computation time. Similar to the modelling approach mentioned above, a 3D Timoshenko beam element (a three-node beam element with consideration of shear flexibility) is used for the rail. The sleeper is assumed to be rigid for Model 3, and is modelled using the 2-node rigid beam elements, as shown in Fig. 3(a). A single element is used for each sleeper and the sleeper mass and rotational inertia act at its centre. A spring-dashpot is applied between rail and sleeper at each of the two rail locations and two spring-dashpots are connected between sleeper and ground, as shown in Fig. 3(a). Two equal loads are applied to the two rails for models 3~4.

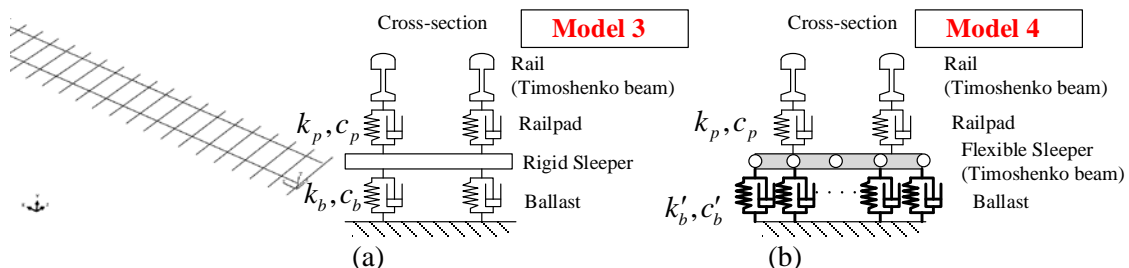


Figure 3: 3D discretely supported rail on spring-dashpots and equivalent multiple spring-dashpot ballast (Models 3 & 4)

Model 4 is similar to Model 3, but instead of using a rigid beam to represent the sleeper, a Timoshenko beam with shear correction factor of 0.85 is used (with 14 spring-dashpots under the sleeper), as shown in Fig. 3(b). The length of the sleeper  $L_{sl}$  is 2.6 m with width  $L_{sw}$  and height  $h_s$  0.25 m and 0.2 m, respectively. Furthermore, the Young's modulus and Poisson's ratio are  $3 \times 10^{10}$  N/m<sup>2</sup> and 0.15, respectively [9].

For Model 5, instead of using multiple spring-dashpot elements to represent the ballast layer, a homogeneous layer accounting for the ballast geometry is considered using 3D eight-node brick element (C3D8), as shown in Fig. 4. The equivalent ballast Young's modulus can be calculated in terms of the ballast geometry by:

$$E_b = 2k_b h_b / [(L_{sw} + c)(w_{b1} + w_{b2})] \quad (3)$$

where,  $w_{b1}$  (1.3 m) and  $w_{b2}$  (1.6 m) are half of the ballast top and bottom dimensions.  $h_b$  (0.3 m) is the height of the ballast layer and  $c$  is a correction factor to allow for load spreading beneath the sleeper in the horizontal direction (along the track).

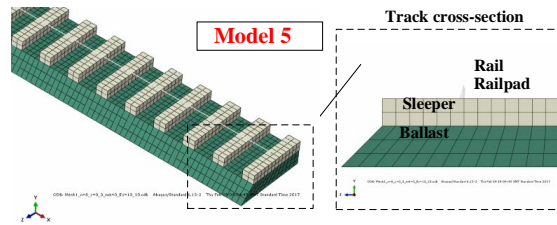


Figure 4: 3D discretely supported rail on homogeneous ballast layer (Model 5)

## 2.3 Models summary

Finally, the equivalent parameters used for the five different numerical models and the analytical model are listed in Table 2. The damping parameters follow a similar transformation as that performed for the stiffness parameters.

Table 2: Equivalent parameter transformation for the analytical model and the five numerical models

	Ballast stiffness input	Units	Railpad stiffness input	Units	Sleeper mass input	Units	Rail mass input	Units
Analytical [5]	$k_b / L_s$	N/m <sup>2</sup>	$k_p / L_s$	N/m <sup>2</sup>	$M_s / (2L_s)$	kg/m	$\rho_r A_r$	kg/m
Model 1	$k_b L_{eff} / L_s$	N/m	$k_p L_{eff} / L_s$	N/m	$M_s L_{eff} / L_s$	kg	$\rho_r A_r L_{eff}$	kg
Model 2	$k_b$	N/m	$k_p$	N/m	$M_s / 2$	kg	$\rho_r A_r$	kg/m
Model 3	$k_b$	N/m	$k_p$	N/m	$M_s$	kg	$\rho_r A_r$	kg/m
Model 4	$2k_b / n_s$	N/m	$k_p$	N/m	$M_s / L_{sl}$	kg/m	$\rho_r A_r$	kg/m
Model 5	Based on $E_b$	N/m <sup>2</sup>	$k_p$	N/m	$M_s / L_{sl}$	kg/m	$\rho_r A_r$	kg/m

\*  $n_s$ : number of nodes for a single sleeper

## 3. Parametric study for modelling guidelines

### 3.1 Results from two-dimensional FE and 2 dof models

#### 3.1.1 Comparison of 2D FE and 2-dof models against analytical solution

Figure 5 shows a comparison of the results between Model 1, Model 2 and the analytical solution in terms of the point receptance above a sleeper. The results from the FE model when 12 rail elements are used per sleeper spacing are virtually identical to those from the analytical solution. Relatively good agreement is found for the 2-dof model up to the second resonance frequency (400 Hz) and

including the first resonance frequency (100 Hz). Poor agreement is found at higher frequencies. Nevertheless, good agreement is found in the vicinity of the second resonance. A good approximation of the receptance is given when the response is stiffness controlled, i.e. below 100 Hz.

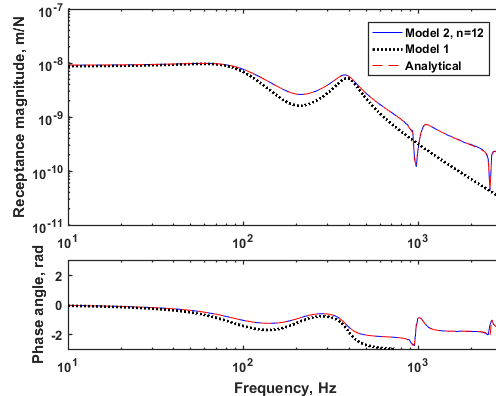


Figure 5: Comparison of rail receptance from Model 1 and Model 2 with analytical results

### 3.1.2 Influence of rail discretisation level

Usually for beams a minimum of six or eight elements are required per propagating wavelength. This gives a maximum element length of:

$$l_e = \left( \frac{1}{N_{element}} \right)^4 \sqrt[4]{\frac{4\pi^2 EI}{m'_r f_{max}^2}} \quad (4)$$

where  $N_{element}$  is the number of elements per wavelength,  $EI$  is the bending stiffness,  $m'_r$  is the mass per unit length and  $f_{max}$  is the maximum frequency of interest. Table 3 shows the percentage difference between the results from Model 2 and the analytical solution when considering different numbers of elements per sleeper spacing. For frequencies up to 800 Hz, the difference is less than 5% based on six elements per wavelength ( $n = 2$ ). However, for frequencies higher than 800 Hz more than 12 elements per wavelength ( $n = 8$ ) are required in order to obtain an error less than 5%. Since the maximum frequency of interest is 2 kHz, according to Table 3, eight elements per sleeper spacing are considered to be sufficient.

Table 3: Percentage difference of receptance magnitude between Model 2 and analytical model at various frequencies

Frequency, Hz	50	100	200	300	400	500	800	1000	2000	3000
Wavelength, m	6.4	4.5	3.2	2.6	2.3	2.0	1.6	1.4	1.0	0.8
$n=1$ (0.65 m)	3.6%	4.5%	6.6%	5.1%	17.8%	46.4%	92.1%	98.1%	44.6%	63.1%
$n=2$ (0.325 m)	0.7%	0.9%	1.4%	1.1%	1.6%	2.5%	3.0%	153.7%	68.8%	19.5%
$n=4$ (0.163 m)	0.0%	0.1%	0.2%	0.1%	0.2%	0.4%	0.3%	27.6%	16.0%	66.2%
$n=6$ (0.108 m)	0.1%	0.1%	0.0%	0.0%	0.0%	0.1%	0.5%	7.2%	7.4%	16.1%
$n=8$ (0.0813 m)	0.1%	0.2%	0.1%	0.1%	0.1%	0.1%	0.6%	0.4%	1.5%	9.2%

### 3.1.3 Influence of model length and boundary effects

Unlike the analytical solution where an infinite rail is considered, the FE model has a limited length, with the boundaries introducing reflections of the waves. As a result, a certain length of track is required to minimise the reflections from both ends of the rail. To assess this, the difference between the results of Model 2 and the analytical solution is calculated for different lengths of the track model. Table 4 lists the maximum frequency for which the error in receptance magnitude is less than 5%. For these track parameters lengths of approximately 10 m, 20 m, and 40 m are required for frequencies up to 500 Hz, 700 Hz, and 2000 Hz, respectively. Additional damping can be applied to reduce the boundary effect [10].

Table 4: Maximum frequency required for different lengths of the track model to give error of less than 5% in receptance magnitude

Model length, m	10.4	20.8	28.6	35.1	42.9
Max. frequency, Hz	500	700	800	850	2000

## 3.2 Results from three-dimensional models

### 3.2.1 Influence of sleeper flexibility

Based on the results from Section 3.1, 67 sleepers with 8 elements per sleeper spacing on the rail are used in Models 3~5. In Models 4 and 5, the element length for the sleeper discretisation is 0.2 m. Fig. 6 shows the results based on a rigid (Model 3) and a flexible sleeper (Model 4), and the analytical solution where a rigid sleeper is used. Good agreement is found between the analytical solution and the model with rigid sleepers, as shown in Fig. 6(a). However, significant differences are found for the second resonance frequency when flexible sleepers are used, as shown in Fig. 6(b). The second resonance frequency tends to reduce, from 385 Hz for the rigid sleeper to 320 Hz for the flexible sleeper. This is due to the influence of the 2<sup>nd</sup> sleeper bending mode, which occurs around 358 Hz here. As it is shown, by increasing the stiffness of the sleeper (10 times higher than the nominal one), the results tend to agree well with the analytical solution.

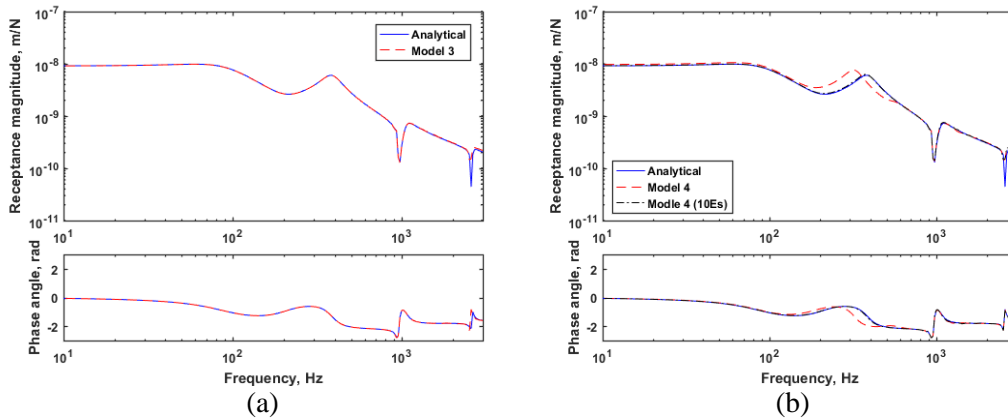


Figure 6: Comparison of the rail receptance: (a) between analytical model and FE model with rigid sleeper; (b) between analytical model and FE model with flexible sleeper

### 3.2.2 Results for different railpad and ballast stiffnesses

Comparison of the results obtained using soft (65 MN/m) and stiff (585 MN/m) railpads while maintaining the same damping ratio are shown in Fig. 7. Differences between the results from Model 3 and Model 4 are very small when softer railpads are used, as shown in Fig. 7(a). On the other hand, increased differences are found between the two different sleeper models with increasing railpad stiffness, as shown in Fig. 7(b). This is because soft railpads allow the rail to vibrate more freely, causing the rail to become decoupled from the sleeper. On the other hand, with stiff railpads the rail is more strongly coupled to the sleeper. In addition, more effects of end reflections can be seen when soft railpads are used; it would require a longer model or additional damping to improve this. Similarly, comparison of the results obtained using soft (32.5 MN/m) and stiff (130 MN/m) ballast while maintaining the same damping ratio are shown in Fig. 8. Similar phenomena are found as for the results based on the original parameters (see Fig. 6(b)). As a result, inclusion of the sleeper flexibility is more influential on the second resonance frequency. At the same time significant differences are found between the results for rigid and flexible sleeper in the case of the stiff railpad, whereas the results are almost identical when soft railpads are used.

### 3.2.3 Investigation of correction factor $c$

Figure 9 shows a comparison of rail receptance between Model 5 using different values for the correction factor  $c$ , with the analytical solution and Model 4. The static stiffness tends to be too high when  $c=0$  compared to the analytical solution, as shown in Fig. 9(a).

Better agreement can be found when  $c=0.4$ . However, the second resonance frequency is lower than the analytical solution. This is again due to consideration of sleeper flexibility as mentioned in Section 3.2.1. Better agreement can be found with Model 4, which considers a flexible sleeper, as shown in Fig. 9(b). However, poor agreement is found between the first resonance and anti-resonance frequency (100~200 Hz). The first resonance frequency from Model 5 is lower than results from Model 4 due to inclusion of the ballast density. Model 5 is the most comprehensive model that should give the closest prediction to real track conditions. As a result, based on the results shown here, an equivalent stiffness for simple track models (Models 1~4) can be derived by using  $c=0.4$ . However, poorer agreement is found at the first resonance frequency due to the omission of ballast density in Models 1~4. This can be improved by increasing the mass attributed to the sleeper.

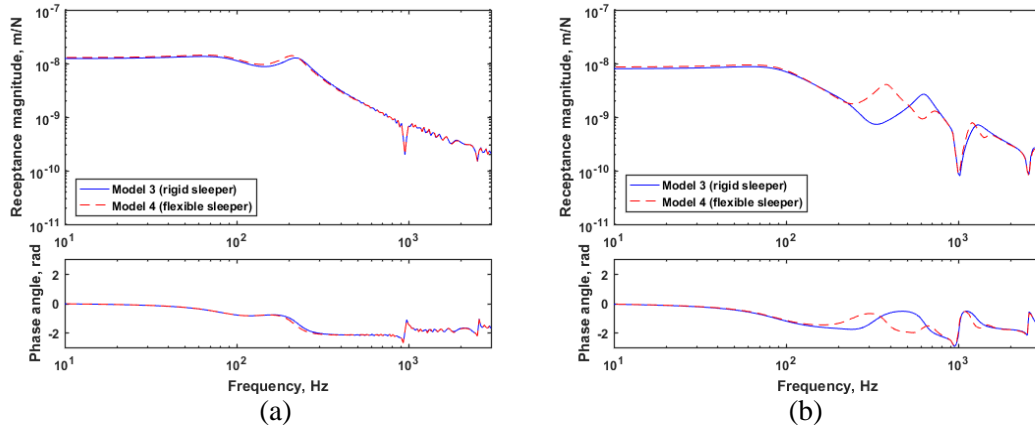


Figure 7: Comparison of rail receptance from rigid sleeper and flexible sleeper with different railpad stiffness; (a)  $k_p=65$  MN/m; (b)  $k_p=585$  MN/m

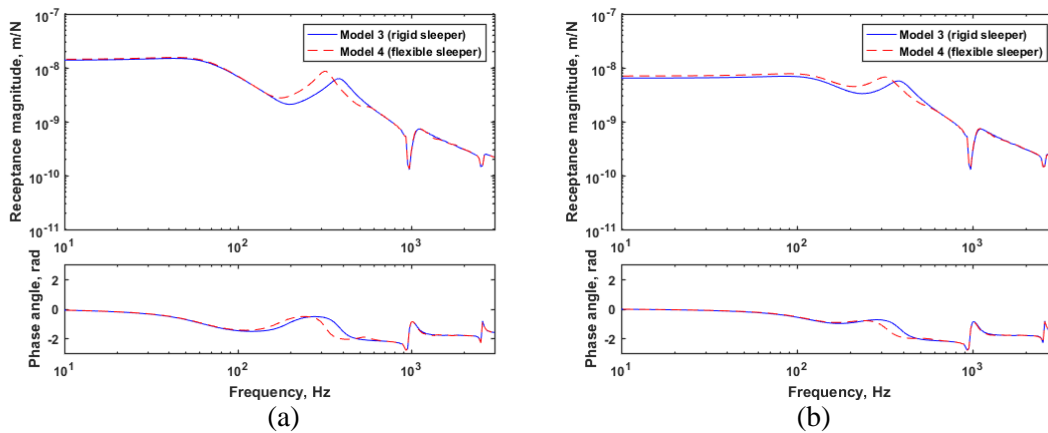


Figure 8: Comparison of rail receptance from rigid sleeper with flexible sleeper with different ballast stiffness (a)  $k_b=32.5$  MN/m; (b)  $k_b=130$  MN/m

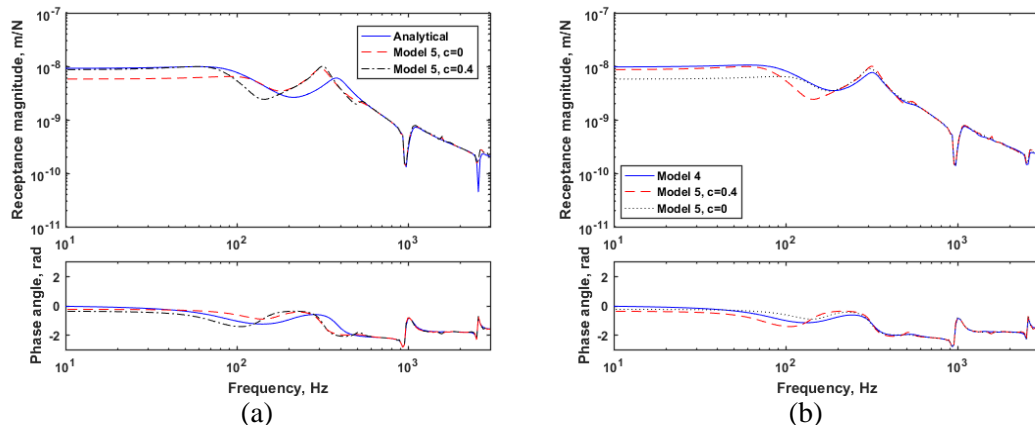


Figure 9: Comparison of rail receptance from Model 5 using different correction factor  $c$  with Model 4 and analytical; (a) comparison with analytical solution; (b) comparison with Model 4

## 4. Efficiency and potential implementation

Table 5 shows the calculation time on the same computer for the five different models for 400 logarithmically spaced frequency points. Clearly, Model 1 is the most efficient. However, poor results are found above the second resonance frequency. Even though Model 2 shows relatively good efficiency and accuracy up to 2 kHz, the flexibility of the sleeper cannot be taken into account. Model 3 also does not consider the flexibility of sleeper and it is more time consuming than Model 2, but it can account for both rails and it would thus be suggested when there is asymmetric loading. Model 4 is less computationally efficient than Model 3, but it accounts for the sleeper flexibility, which has a significant influence for the second resonance frequency especially for stiff rail pads. Model 5 is the most computationally demanding model of all. However, ballast density can be included, which plays an important role for the first resonance frequency. Furthermore, a more complicated model can be implemented such as an elastoplastic model for the ballast, which can be used to predict ballast settlement.

Table 5: Number of degrees of freedom in each model and CPU time required to calculate rail receptance

	Model 1	Model 2	Model 3	Model 4	Model 5
CPU time (s)	0.01	21.7	56.0	84.4	3047
Degrees of freedom	2	3,710	15,644	24,488	175,524

## 5. Conclusion

A significant benefit in terms of efficiency is found using a 2-dof track model. Even though poor agreement is found at higher frequency between this model and a flexible track, good agreement is shown up to and including the second resonance frequency, here around 400 Hz. Even though consideration of flexible sleepers has a significant influence on the second resonance frequency, it can be neglected when soft railpads are used. Finally, simple guidelines are proposed to obtain the correct parameter transformation from the more advanced models to the simpler ones.

## REFERENCES

- 1 S. Iwnicki, Handbook of Railway Vehicle Dynamics, CRC Press, (2006).
- 2 E. Di Gialleonardo, F. Braghin, S. Bruni, The influence of track modelling options on the simulation of rail vehicle dynamics, *J. Sound Vib.*, 331, 4246–4258, (2012).
- 3 I. Kaiser, Refining the modelling of vehicle–track interaction, *Veh. Syst. Dyn.*, 50, 229–243, (2012).
- 4 G. Kouroussis, O. Verlinden, C. Conti, A two-step time simulation of ground vibrations induced by the railway traffic, *Proc. Inst. Mech. Eng. Part C J. Mech. Eng. Sci.*, 226, 454–472, (2011).
- 5 D.J. Thompson, *Railway Noise and Vibration, Mechanisms, Modelling and Means of Control*, Elsevier Ltd, (2009).
- 6 K.L. Knothe, S.L. Grassie, Modelling of railway track and vehicle/track interaction at high frequencies, *Veh. Syst. Dyn.*, 22, 209–262, (1993).
- 7 H.H. Jenkins, J.E. Stephenson, G.A. Clayton, D. Lyon, The effect of track and vehicle parameters on wheel/rail vertical dynamic loads, *J. Railw. Eng. Soc.*, 3, 2–16, (1974).
- 8 J. Yang, D.J. Thompson, Y. Takano, Characterizing wheel flat impact noise with an efficient time domain model, *Noise Vib. Mitig. Rail Transp. Syst.*, 126, 109–116, (2015).
- 9 RIVAS Project, Results of the parameter studies and prioritization for prototype construction for ballasted track, (2012).
- 10 J. Yang, D.J. Thompson, A non-reflecting boundary for use in a finite element beam model of a railway track, *J. Sound Vib.*, 337, 199–217, (2015).